Lattice Dynamics and Superconductivity in Cerium at High Pressure

I. Loa,[1,*] E. I. Isaev,[2,3] M. I. McMahon,[1] D. Y. Kim,[4,†] B. Johansson,[4,5] A. Bosak,[6] and M. Krisch[6]

[1]*SUPA, School of Physics and Astronomy, and Centre for Science at Extreme Conditions, The University of Edinburgh,
Edinburgh, United Kingdom*
[2]*Department of Physics, Linköping University, Linköping, Sweden*
[3]*Theoretical Physics Department, National University of Science and Technology "MISIS," Moscow, Russia*
[4]*Department of Physics, Uppsala University, Uppsala, Sweden*
[5]*Department of Materials and Engineering, Royal Institute of Technology, Stockholm, Sweden*
[6]*European Synchrotron Radiation Facility, Grenoble, France*

We have measured phonon dispersion relations of the high-pressure phase cerium-$oC4$ (α' phase with the α-uranium crystal structure) at 6.5 GPa by using inelastic x-ray scattering. Pronounced phonon anomalies are observed, which are remarkably similar to those of α-U. First-principles electronic structure calculations reproduce the anomalies and allow us to identify strong electron-phonon coupling as their origin. At the low-pressure end of its stability range, Ce-$oC4$ is on the verge of a lattice-dynamical instability and possibly a charge density wave. The superconducting transition temperatures of the fcc, $oC4$, and $mC4$ phases of Ce have been calculated, and the superconductivity observed experimentally by Wittig and Probst is attributed to the $oC4$ phase.

PACS numbers: 63.20.D−, 62.50.−p, 71.15.Mb, 78.70.Ck

Cerium is an element with most unusual properties. It is perhaps best known for its pressure- and temperature-induced isostructural transition between two phases (γ and α), where the face-centered-cubic (fcc) crystal structure is preserved, but the atomic volume changes by $\sim 15\%$ at 0.8 GPa and room temperature [1,2]. The physics of this transition has been, and is to this day, intensely debated. The $4f$ electrons play a central role, but to what extent this phenomenon is driven by electron delocalization, changes in electronic screening, and vibrational entropy, and whether it is better described as a Mott or as a Kondo transition, is still a matter of dispute and ongoing research (see [3–8], and references therein).

Upon further compression to 5–6 GPa at room temperature, Ce transforms from the collapsed α-fcc phase to one of two different phases (α' or α''), depending on the mechanical treatment of the starting material and the rate of pressure increase [9,10]. The α' phase has an orthorhombic crystal structure with space group $Cmcm$ (Pearson symbol $oC4$), and it is isostructural with α-uranium (Fig. 1). The α'' ($mC4$) phase has a monoclinic crystal structure with space group $C2/m$ [10]. In this study, we have taken advantage of a peculiarity of the fcc $\rightarrow oC4$ transition: Upon slow increase of pressure under sufficiently hydrostatic conditions, a grain of fcc-Ce with a polycrystalline microstructure usually transforms into a single crystal of $oC4$-Ce [10,11], even at ambient temperature, which is ~ 700 K below the melting temperature.

Uranium adopts the same $oC4$ crystal structure at ambient conditions, but, upon cooling below 43 K, an incommensurate modulation of the structure, a charge density wave (CDW), develops [12]. Further transitions occur at lower temperatures, where the components of the modulation vector successively lock in at commensurate values [13–15]. Fast *et al.* [16] identified the Peierls-type opening of partial gaps of electronic bands at the Fermi level as the origin of the CDW and pointed out the strong Fermi-surface nesting of narrow bands with predominantly f character.

The unmodulated $oC4$ crystal structure has been reported to exist also for high-pressure phases of the lanthanides Pr and Nd [17,18] as well as the actinide Pa [19], while reports for other actinides have later been revised [20]. Uranium is so far the only element with the $oC4$ crystal structure where the lattice dynamics has been investigated and a CDW has been observed. α-U exhibits pronounced phonon anomalies and temperature-dependent mode softening, which leads eventually to the formation of the CDW [12,21,22]. The possibility to grow high-quality single crystals of Ce-$oC4$ at high pressure offers a unique opportunity to study, experimentally, the lattice dynamics in a system with the same crystal structure as α-U but a very different electronic structure, to explore the
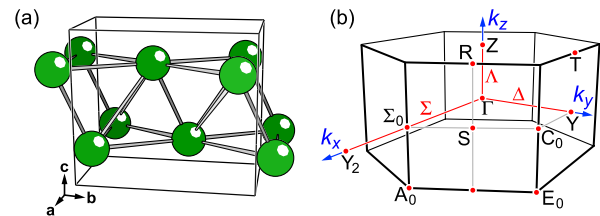

FIG. 1 (color online). (a) Crystal structure and (b) Brillouin zone of Ce-$oC4$ (α-U type). Cell boundaries are indicated by black lines, and the near-neighbor contacts are highlighted in (a).

possibility of a CDW in Ce, and to provide accurate experimental data as a test bed for the ongoing efforts to model the electronic structure and properties of Ce.

Using inelastic x-ray scattering (IXS), we have measured phonon dispersion relations of Ce-$oC4$ at 6.5 GPa ($T = 295$ K). Pronounced phonon anomalies are observed that bear many similarities with those of α-U. We will present results of extensive first-principles electronic structure calculations to identify the origin of the anomalies and to answer the long-standing question of which of the two competing phases of Ce above 4 GPa gives rise to the experimentally observed superconductivity with $T_c \approx$ 2 K [23–25].

The IXS experiments were performed on beam line ID28 at the European Synchrotron Radiation Facility, Grenoble with a photon energy of 17.794 keV and an energy resolution of 3 meV [26,27]. Single crystals of the phase Ce-$oC4$ were obtained as described previously [10] in Merrill-Bassett-type diamond anvil high-pressure cells with a 4:1 methanol/ethanol mixture as the pressure-transmitting medium [26]. Density functional theory and the linear response method [28] as implemented in the QUANTUM ESPRESSO code [29] were used to calculate phonon dispersion relations and electron-phonon coupling constants. An ultrasoft pseudopotential with the valence configuration $5s^2 5p^6 5d^1 6s^2 4f^1$ (i.e., with explicitly included f electrons) was employed, and exchange-correlation effects were treated within the generalized-gradient approximation [30]. Additional density functional theory calculations were performed with the full-potential augmented-plane-wave plus local orbital method as implemented in the WIEN2K code [31] to analyze the electronic band structure and Fermi surface of Ce-$oC4$. The $5s$, $5p$, $5d$, $6s$, and $4f$ orbitals were treated as valence states, and the generalized-gradient approximation was used [26].

IXS data of Ce-$oC4$ were collected along the high-symmetry directions [$\zeta00$], [$0\zeta0$], and [00ζ] (Σ, Δ, and Λ), and selected spectra are shown in Fig. 2. Various scattering geometries were chosen on the basis of preliminary phonon calculations so as to optimize the intensity and contrast of individual phonon branches in the experiment. Also shown in Fig. 2 are decompositions of the measured spectra into the elastic line, the excitation peaks, and a constant background that were obtained by least-squares fitting [26].

Figure 3(a) depicts the phonon dispersion relations as determined from the dominant peaks in the IXS spectra. The lowest-energy optical branch along Γ-Y (Σ_4) is unusually low in energy relative to the acoustic branches, and it exhibits a pronounced dip near ($\frac{1}{2}00$). The Σ_1 acoustic branch is also anomalous near ($\frac{1}{2}00$), and further anomalies exist at other wave vectors, e.g., the depressions of the Σ_4 and Σ_1 branches at the Y point and of the Σ_4 branch at Γ.

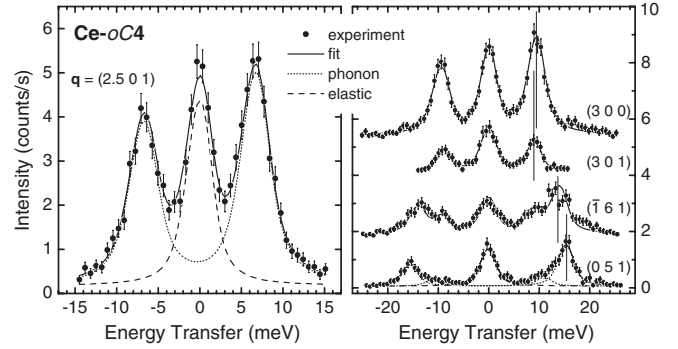Overall, these phonon anomalies are remarkably similar to those observed for α-U at ambient conditions [21]. In

FIG. 2. Selected IXS spectra of Ce-$oC4$ at 6.5 GPa for different momentum transfers **q**. When **q** is reduced to the first Brillouin zone, (2.5 0 1) corresponds to ($\frac{1}{2}00$), i.e., halfway along the Γ-Y line. The spectra in the right panel are collected with momentum transfers all corresponding to the Y point (100) but with emphasis on different phonon branches. The spectra are offset vertically for clarity.

α-U, the dip of the Σ_4 branch near ($\frac{1}{2}00$) exhibits soft-mode behavior with decreasing temperature [12] and pressure [32,33], and this dip represents a saddle point in three dimensions. The minima are located at $\mathbf{q}_{min} = (\pm0.49, \pm0.13, \pm0.21)$ at 55 K [22], and the mode softening at these positions results in the formation of the CDW below 43 K. It would have been desirable to follow the phonon anomalies in Ce to lower pressure and/or low temperature, but this has experimentally not been feasible. We did perform a preliminary single-crystal x-ray diffraction experiment on Ce-$oC4$ at 8.5 GPa and low temperature in search of superlattice reflections—but did not find any evidence thereof down to 20 K.

In order to understand the origin of the observed phonon anomalies and to explore the properties of Ce-$oC4$ at lower pressures, we have calculated the phonon dispersion relations of Ce-$oC4$ at pressures of 6.5, 4, and 2 GPa ($T =$ 0 K), and the main results are shown in Fig. 3(b). Bearing in mind that the $4f$ electrons were treated as "standard" valence electrons (i.e., without considering electron-electron correlations beyond the generalized-gradient approximation), the overall agreement between theory and experiment is quite satisfactory. The essence of the lattice dynamics of Ce-$oC4$ is captured by the calculations, and the anomalies of the Σ_4 and Σ_1 branches are reproduced. The calculations show that both these branches have longitudinal character; i.e., the atomic displacements are approximately parallel to [100], as in α-U. The most notable deviations between theory and experiment occur for the lowest-energy optical branches Δ_4 and Λ_2, which have again atomic displacements parallel to [100]. The cause of these deviations is presently unclear, but it is remarkable that a recent lattice-dynamical study of α-U shows very similar deviations for the same branches [32].

Figure 3(b) also shows that reducing the pressure from 6.5 GPa renders the ($\frac{1}{2}00$) anomaly of the Σ_4 branch more
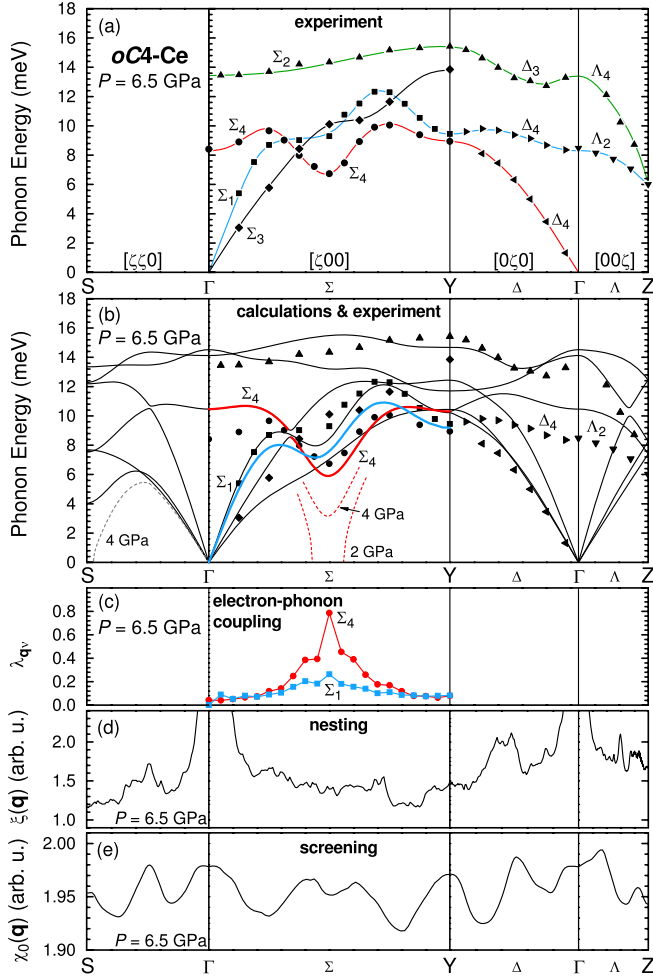
FIG. 3 (color online). (a) Experimental phonon dispersion relations for Ce-$oC4$ at 6.5 GPa. The symbols distinguish **q** scans with different momentum offsets relative to the center of the Brillouin zone: ▲ (151)–(051)–(041)–(04$\frac{1}{2}$); ● (201)–(301); ■ (200)–(300); ◆ (061)–($\bar{1}$61); ▶ (210)–(220); ◀ (210)–(200); ▼ (201)–(20$\frac{1}{2}$). The experimental uncertainties of the phonon energies correspond approximately to the symbol size. The lines are guides to the eye, and the branches are labeled as in Ref. [21]. (b) Calculated phonon energies (solid lines) and IXS results (symbols). Selected results of the calculations at 4 and 2 GPa are indicated by dashed lines. (c) Mode-specific electron-phonon coupling strength $\lambda_{\mathbf{q}\nu}$ for the Σ_4 and Σ_1 branches. (d) Fermi-surface nesting function $\xi(\mathbf{q})$. (e) Bare static susceptibility $\chi_0(\mathbf{q})$.

pronounced in the calculations, and this branch becomes unstable below 3 GPa. The calculations indicate additional strong anomalies for several branches near the S point of the Brillouin zone [$\mathbf{q} = (\frac{1}{2}\frac{1}{2}0)$], with one of the acoustic branches being unstable below 4.3 GPa. As Ce-$oC4$ has been observed experimentally down to at least 3.6 GPa upon pressure release at low temperature [24], there is the possibility of the formation of a superstructure or charge density wave in Ce at around 4 GPa and at low temperature, but this awaits experimental investigation.

In a metal, phonon anomalies as observed for Ce are often caused by the electron-phonon interaction, and we have therefore examined various factors that contribute to the electron-phonon coupling. We start from the phonon self-energy for a phonon of energy ω, wave vector **q**, and branch index ν [34]:

$$\mathbf{\Pi}(\mathbf{q}, \nu, \omega) = -\frac{2}{N_k} \sum_{\mathbf{k}nm} \frac{f(\epsilon_{\mathbf{k}n}) - f(\epsilon_{\mathbf{k}+\mathbf{q}m})}{\epsilon_{\mathbf{k}+\mathbf{q}m} - \epsilon_{\mathbf{k}n} - \hbar\omega - i\delta}$$
$$\times |M^{[\nu]}_{\mathbf{k}n,\mathbf{k}+\mathbf{q}m}|^2,$$

where N_k is the number of k points in the summation, f the Fermi-Dirac distribution function, $\epsilon_{\mathbf{k}n}$ the energy of the electronic state of wave vector **k** and band index n, and $M^{[\nu]}_{\mathbf{k}n,\mathbf{k}+\mathbf{q}m}$ the electron-phonon matrix element, and the self-energy is evaluated for $\delta \to 0$. The real part of the complex self-energy describes the renormalization of the phonon energy, i.e., the phonon softening, while the imaginary part yields the mode-specific electron-phonon coupling strength $\lambda_{\mathbf{q}\nu}$. The calculated $\lambda_{\mathbf{q}\nu}$ are shown in Fig. 3(c) for the anomalous Σ_4 and Σ_1 branches. The Σ_4 branch exhibits strong coupling with a maximum $\lambda_{\mathbf{q}\nu} \gtrsim$ 0.79 near ($\frac{1}{2}$00), and the Σ_1 branch also shows a pronounced maximum with $\lambda_{\mathbf{q}\nu} \gtrsim 0.26$. The coupling strengths for the other branches (not shown) are weaker (< 0.15) and exhibit little wave-vector dependence.

To assess the importance of the Fermi-surface properties, we consider now the coupling strength in the limit $\omega \to 0$:

$$\lambda_{\mathbf{q}, \nu} = \frac{1}{N(0)\omega_{\mathbf{q},\nu}} \frac{2}{N_k} \sum_{\mathbf{k}nm} |M^{[\nu]}_{\mathbf{k}n,\mathbf{k}+\mathbf{q}m}|^2 \delta(\epsilon_{\mathbf{k}n})\delta(\epsilon_{\mathbf{k}+\mathbf{q}m}),$$

where $N(0)$ is the electronic density of states at the Fermi level ($E_F = 0$) and δ the Dirac δ function. The two important contributions are the matrix elements $M^{[\nu]}_{\mathbf{k}n,\mathbf{k}+\mathbf{q}m}$ and the Fermi-surface nesting function $\xi(\mathbf{q}) = (2/N_k)\sum_{\mathbf{k}nm}\delta(\epsilon_{\mathbf{k}n})\delta(\epsilon_{\mathbf{k}+\mathbf{q}m})$, which quantifies the overlap of the Fermi surface with an image of itself that is shifted by a vector **q**.

The calculated Fermi surface of Ce-$oC4$ at 6.5 GPa is shown in Fig. 4. It is derived predominantly from states with $4f$ character and smaller contributions from $5d$ states. The Fermi surface has a complex topology that does not lend itself to effective nesting. Unsurprisingly, therefore, the nesting function shown in Fig. 3(d) does not exhibit any particularly strong features (except for the trivial maximum at $\mathbf{q} = 0$), and the discernible peaks represent nesting of only a few percent of the Fermi surface. The strong electron-phonon coupling of the Σ_4 and Σ_1 branches near ($\frac{1}{2}$00) is therefore due to large matrix elements and not caused by Fermi-surface nesting.

The final element to consider is the bare static susceptibility $\chi_0(\mathbf{q}) = (2/N_k)\sum_{\mathbf{k}nm}[f(\epsilon_{\mathbf{k}n}) - f(\epsilon_{\mathbf{k}+\mathbf{q}m})]/[\epsilon_{\mathbf{k}+\mathbf{q}m} - \epsilon_{\mathbf{k}n}]$, which describes the wave-vector-dependent screening of the electrostatic forces by the
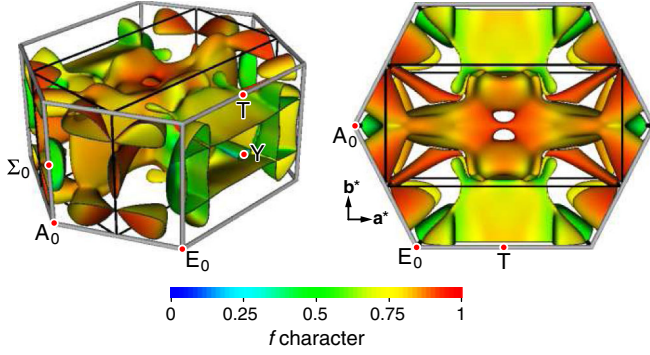
FIG. 4 (color online). Calculated Fermi surface of Ce-$oC4$ at 6.5 GPa. Colors represent the f character of the electronic states at the Fermi level, according to the angular decomposition of the wave functions in the atomic spheres. Thick gray lines show the edges of the Brillouin zone, while the black lines mark the Wigner-Seitz cell corresponding to the conventional crystallographic unit cell.

conduction electrons in a metal. Phonon softening—Kohn anomalies—can occur at wave vectors where $\chi_0(\mathbf{q})$ has maxima. Figure 3(e) shows that there exist several peaks in the susceptibility along the high-symmetry lines. There is, in particular, a pronounced peak at the Y point, where the Σ_4 and Σ_1 branches have pronounced dips. Altogether, we identify strong electron-phonon coupling due to large electron-phonon matrix elements as the origin of the pronounced dips of the Σ_4 and Σ_1 phonon branches near $\mathbf{q} = (\frac{1}{2}00)$, while the weaker anomalies, e.g., at the Y point, can best be understood as Kohn anomalies resulting from maxima in the susceptibility.

The results on strong electron-phonon coupling immediately point at the possibility of superconductivity in Ce-$oC4$. In extension of the above calculations, we have estimated the superconducting transition temperatures T_c of Ce at 6.5 GPa for three crystal structures—fcc, orthorhombic $oC4$, and monoclinic $mC4$—by using the Allen-Dynes formula [35] with a Coulomb potential parameter of $\mu^* = 0.11$. The electron-phonon coupling in the fcc and $mC4$ phases is marginal, and we obtained $T_c \approx 1$ K. For Ce-$oC4$ at 6.5 GPa, we obtained $T_c = 4.5$ K, and this value increases slightly to 5.1 K when the pressure is reduced to 4.6 GPa.

Experimental data on the superconductivity in Ce are surprisingly scarce. Wittig reported the observation of superconductivity in Ce above 5 GPa with $T_c \approx 1.5$ K [23]. Subsequent work showed a slight increase of T_c to 1.9 K when the pressure is lowered to 3.6 GPa, where a phase transition occurred [24,25]. It has remained unclear whether the observed superconductivity is a property of the $oC4$ or the $mC4$ phase (or both), as both phases can be obtained above 5 GPa. Superconductivity in fcc-Ce was detected only at pressures above 2 GPa and with a very low T_c of less than 0.05 K [25].

The comparison of the calculated and experimental results indicates that (i) our calculations slightly overestimate T_c (but the agreement can be improved by choosing a larger μ^*), that (ii) the monoclinic $mC4$ phase is at best marginally superconducting like the fcc phase, and, most importantly, that (iii) the superconductivity observed in Ce at pressures above ~5 GPa can be attributed to the orthorhombic $oC4$ phase.

For comparison, α-U is also superconducting, with a maximum T_c of 2.4 K at 1.2 GPa—where its CDW appears to be suppressed—and a somewhat lower T_c down to 0.5 K in the modulated phases [15,36]. We have already pointed out how similar the phonon anomalies—and the deviations between computational and experimental results—are for the two elements. Overall, the similarities between the $oC4$ phases of Ce and U are quite striking, considering their different electronic configurations. It is therefore interesting to note that unusual vibrational properties have been reported for U at elevated temperatures at around 500 K, where a large thermal softening was observed in the phonon density of states [37], which appears to relate to an abrupt loss in scattering intensity for an optical branch and the concomitant appearance of a new dynamical mode [38]. The nature of this new mode is not yet fully understood; it was initially interpreted as an "intrinsically localized vibration" originating from anharmonic interactions [38], but an alternative model based on strong electron-phonon interaction together with low-energy excitations of the f electrons was recently put forward [39]. If future high-temperature studies on Ce were to find evidence of similar effects, this would provide a valuable contribution both to understanding the nature of the new dynamical mode and to the ongoing Mott-versus-Kondo debate for Ce.

In summary, we have measured phonon dispersion relations of Ce-$oC4$ at high pressure by using IXS and observed pronounced anomalies, which are surprisingly similar to those in α-U, given the very different electronic configurations of the two elements. The anomalies in Ce originate from strong electron-phonon coupling, with the matrix-element contributions being dominant for some modes, while others are of the Kohn type. At ~4 GPa, Ce-$oC4$ is at the verge of a dynamical instability. The superconductivity observed experimentally by Wittig and Probst with $T_c \approx 2$ K can be attributed to the $oC4$ phase. Our experimental results provide a stringent test for the continued efforts to model the electronic structure and properties of Ce. By treating the cerium $4f$ electron as itinerant, we reproduce the experimental phonon data in Ce equally well as previously for U [32] when the $5f$ electrons were included as part of the conduction band. It appears worthwhile to examine in future work why Ce and U show these anomalies, while Pa (uranium's heavier neighbor in the periodic table) has been predicted not to exhibit them [32] and to extend the experiments to elevated temperatures.

*Corresponding author.
I.Loa@ed.ac.uk
†Present address: Geophysical Laboratory, Carnegie Institution of Washington, Washington, DC, USA.

[1] P. Bridgman, Proc. Am. Acad. Arts Sci. **62**, 207 (1927).

[2] A. W. Lawson and T.-Y. Tang, Phys. Rev. **76**, 301 (1949).

[3] B. Johansson, Philos. Mag. **30**, 469 (1974); Phys. Rev. B **11**, 2740 (1975).

[4] J. W. Allen and R. M. Martin, Phys. Rev. Lett. **49**, 1106 (1982); J. W. Allen and L. Z. Liu, Phys. Rev. B **46**, 5047 (1992).

[5] M. Lavagna, C. Lacroix, and M. Cyrot, Phys. Lett. **90A**, 210 (1982).

[6] B. Johansson, I. A. Abrikosov, M. Aldén, A. V. Ruban, and H. L. Skriver, Phys. Rev. Lett. **74**, 2335 (1995).

[7] I.-K. Jeong, T. W. Darling, M. J. Graf, T. Proffen, R. H. Heffner, Y. Lee, T. Vogt, and J. D. Jorgensen, Phys. Rev. Lett. **92**, 105702 (2004).

[8] M. Krisch et al., Proc. Natl. Acad. Sci. U.S.A. **108**, 9342 (2011).

[9] F. H. Ellinger and W. H. Zachariasen, Phys. Rev. Lett. **32**, 773 (1974).

[10] M. I. McMahon and R. J. Nelmes, Phys. Rev. Lett. **78**, 3884 (1997).

[11] G. Gu, Y. K. Vohra, and K. E. Brister, Phys. Rev. B **52**, 9107 (1995).

[12] H. G. Smith, N. Wakabayashi, W. P. Crummett, R. M. Nicklow, G. H. Lander, and E. S. Fisher, Phys. Rev. Lett. **44**, 1612 (1980).

[13] J. C. Marmeggi, G. H. Lander, S. van Smaalen, T. Brückel, and C. M. E. Zeyen, Phys. Rev. B **42**, 9365 (1990).

[14] G. Grübel, J. D. Axe, D. Gibbs, G. H. Lander, J. C. Marmeggi, and T. Brückel, Phys. Rev. B **43**, 8803 (1991).

[15] G. Lander, E. Fisher, and S. Bader, Adv. Phys. **43**, 1 (1994).

[16] L. Fast, O. Eriksson, B. Johansson, J. M. Wills, G. Straub, H. Roeder, and L. Nordström, Phys. Rev. Lett. **81**, 2978 (1998).

[17] G. S. Smith and J. Akella, J. Appl. Phys. **53**, 9212 (1982).

[18] G. N. Chesnut and Y. K. Vohra, Phys. Rev. B **61**, R3768 (2000).

[19] R. G. Haire, S. Heathman, M. Idiri, T. Le Bihan, A. Lindbaum, and J. Rebizant, Phys. Rev. B **67**, 134101 (2003).

[20] K. T. Moore and G. van der Laan, Rev. Mod. Phys. **81**, 235 (2009).

[21] W. P. Crummett, H. G. Smith, R. M. Nicklow, and N. Wakabayashi, Phys. Rev. B **19**, 6028 (1979).

[22] J.-C. Marmeggi, G. H. Lander, A. Bouvet, and R. Currat, J. Phys. Conf. Ser. **92**, 012173 (2007).

[23] J. Wittig, Phys. Rev. Lett. **21**, 1250 (1968).

[24] C. Probst and J. Wittig, Ferroelectrics **16**, 267 (1977).

[25] C. Probst and J. Wittig, in Proceedings of the 14th International Conference on Low Temperature Physics, Otaniemi, Finland, edited by M. Krusius and M. Vuorio (North-Holland, Amsterdam, 1975), Vol. 5, pp. 453–456.

[26] See Supplemental Material at http://link.aps.org/supplemental/10.1103/PhysRevLett.108.045502 for full technical details.

[27] M. Krisch, J. Raman Spectrosc. **34**, 628 (2003).

[28] S. Baroni, S. de Gironcoli, A. Dal Corso, and P. Giannozzi, Rev. Mod. Phys. **73**, 515 (2001).

[29] P. Giannozzi et al., J. Phys. Condens. Matter **21**, 395502 (2009), http://www.quantum-espresso.org.

[30] J. P. Perdew, K. Burke, and M. Ernzerhof, Phys. Rev. Lett. **77**, 3865 (1996).

[31] P. Blaha, K. Schwarz, G. K. H. Madsen, D. Kvasnicka, and J. Luitz, WIEN2K, An Augmented Plane Wave + Local Orbitals Program for Calculating Crystal Properties (K. Schwarz, Technische Universität Wien, Austria, 2001).

[32] J. Bouchet, Phys. Rev. B **77**, 024113 (2008).

[33] S. Raymond et al., Phys. Rev. Lett. **107**, 136401 (2011).

[34] W. E. Pickett and P. B. Allen, Phys. Rev. B **16**, 3127 (1977).

[35] P. B. Allen and R. C. Dynes, Phys. Rev. B **12**, 905 (1975).

[36] T. F. Smith and E. S. Fisher, J. Low Temp. Phys. **12**, 631 (1973).

[37] M. E. Manley, B. Fultz, R. J. McQueeney, C. M. Brown, W. L. Hults, J. L. Smith, D. J. Thoma, R. Osborn, and J. L. Robertson, Phys. Rev. Lett. **86**, 3076 (2001).

[38] M. E. Manley, M. Yethiraj, H. Sinn, H. M. Volz, A. Alatas, J. C. Lashley, W. L. Hults, G. H. Lander, and J. L. Smith, Phys. Rev. Lett. **96**, 125501 (2006).

[39] X. Yang and P. S. Riseborough, Phys. Rev. B **82**, 094303 (2010).

[40] http://www.ecdf.ed.ac.uk

[41] http://www.edikt.org.uk